



ELSEVIER

Journal of Alloys and Compounds 300–301 (2000) 207–213

Journal of  
ALLOYS  
AND COMPOUNDS

www.elsevier.com/locate/jallcom

# Luminescence characteristics of Er-doped GaN semiconductor thin films

J.M. Zavada<sup>a,\*</sup>, Myo Thaik<sup>b</sup>, U. Hömmerich<sup>b</sup>, J.D. MacKenzie<sup>c</sup>, C.R. Abernathy<sup>c</sup>, S.J. Pearton<sup>c</sup>, R.G. Wilson<sup>d</sup>

<sup>a</sup>European Research Office, London, NW1 5TH, UK

<sup>b</sup>Hampton University, Hampton, VA 23668, USA

<sup>c</sup>University of Florida, Gainesville, FL 32611, USA

<sup>d</sup>Stevenson Ranch, CA 91381, USA

## Abstract

Semiconductors doped with rare earth atoms have been studied for more than a decade because of the potential of using them to develop compact and efficient electroluminescence (EL) devices. Trivalent erbium ions ( $\text{Er}^{3+}$ ) are of special interest because they exhibit atomic-like transitions centered at 1540 nm, which corresponds to the low-loss window of silica-based optical fibers. While EL devices, based on Er-doped Si and GaAs materials, have been fabricated, their efficiency remains too low for practical applications. Several years ago an important observation was made that there was less detrimental temperature quenching of Er luminescence intensity for larger bandgap host materials. Therefore, Er-doping of wide gap semiconductors, such as the III–V nitrides, appears to be a promising approach to overcoming the thermal quenching of Er luminescence found in Si and GaAs. In particular, GaN epilayers doped with Er ions have shown a highly reduced thermal quenching of the intensity of the Er luminescence from cryogenic to elevated temperatures. The remarkable thermal stability of the light emission may be due to the large energy bandgap of the material, as well as to the optical inactivity of the material defects in the GaN films. In this paper, recent data concerning the luminescence characteristics of Er-doped GaN thin films are presented. Two different methods have been used for Er-doping of the GaN films: ion implantation and in situ doping during epitaxial growth. Both methods have proven successful for incorporation and optical activation of  $\text{Er}^{3+}$  ions. Infrared photoluminescence spectra, centered at 1540 nm, have been measured for various Er-doped III–N films. Considerably different emission spectra, with different thermal quenching characteristics, have been observed, depending upon the wavelength of the optical pump and the Er-doping method. Defect-related absorption centers permit excitation of the Er ions using below-bandgap optical sources. Elemental impurities, such as O and C, in the thin films have also been shown to influence the emission spectra and to lead to different optical characteristics. © 2000 Published by Elsevier Science S.A. All rights reserved.

**Keywords:** Rare earths; Photoluminescence; Electroluminescence; GaN; Er doping

## 1. Er-doping of semiconductors

The optical properties of rare earth ions in insulating materials have been extensively studied for applications in solid-state lasers and optical fiber amplifiers [1]. Solid-state lasers, such as  $\text{Nd}^{3+}$ :YAG, are based on the 4*f* intra-subshell transitions of the rare earth trivalent ions ( $\text{RE}^{3+}$ ) and exhibit a very stable lasing wavelength with a minimum temperature dependence. Because of these characteristics, such lasers have found widespread applications in laboratory and military systems. Er-doped silica fibers are being used for amplification of optical signals in wavelength division multiplexing (WDM) communication systems operating at 1.54  $\mu\text{m}$  [2]. Pr-doped fibers are

being developed for similar optical amplification at 1.3  $\mu\text{m}$ .

Investigations of the optical properties of rare earth-doped III–V semiconductors have been studied for over a decade. Beginning with the work of Ennen et al. in 1983 [3], the luminescence of rare earth ions in III–V compound semiconductors has received considerable attention. The main goal of this work has been to develop electrically pumped optical sources and amplifiers for use in optical communication systems. Studies of rare earth ions in a variety of different semiconductors have been conducted [4–6]. Due to the importance of the 1.54  $\mu\text{m}$  region for optical communications, Er has been the main rare earth element to be investigated. Si has been the primary semiconductor host for these investigations because of its predominance in the microelectronics industry. However, several barriers have hindered the development of Er-

\*Corresponding author.

E-mail address: jzavada@army.ehis.navy.mil (J.M. Zavada)

doped Si optoelectronics. Incorporation of Er atoms in the Si crystal is limited to approximately  $10^{18} \text{ cm}^{-3}$ . Above that level Er clusters occur and infrared light emission is reduced. In addition, the intensity of the Er emission decreases significantly as the temperature of the Er-doped Si wafer increases from cryogenic to room temperatures.

Favennec et al. studied the dependence of the emission intensity of the  $\text{Er}^{3+}$  ions on the bandgap of the host semiconductor as a function of sample temperature [7]. Several different semiconductors, including Si, were implanted with  $\text{Er}^+$  ions and the emission intensity was measured at different temperatures. It was found that the photoluminescence (PL) intensity decreased at higher temperatures. This thermal quenching of the PL intensity was more severe for the smaller bandgap materials, such as Si (1.12 eV) and GaAs (1.43 eV). The wider bandgap compounds, such as ZnTe (2.26 eV) and CdS (2.42 eV), exhibited less temperature dependence.

Since wider bandgap semiconductors lead to less thermal quenching of the  $\text{Er}^{3+}$  PL intensity, the III–V nitride alloys appear to be especially promising host materials for rare earth doping. These alloys have a direct bandgap ranging from 1.9 eV for InN to 3.4 eV for GaN and 6.2 eV for AlN. However, due to a lack of a lattice matched substrate, most III–V nitride epilayers are grown on sapphire ( $\text{Al}_2\text{O}_3$ ) or SiC substrates and contain a high density of dislocation defects. High levels of various impurity elements, such as C or O or H, are also found in many nitride epilayers. Nevertheless, very encouraging results have been obtained with Er-doped III–V nitride materials.

The main methods for incorporating Er atoms into III–V semiconductor materials have been ion implantation and in situ doping during epitaxial growth. Each method presents certain advantages as well as difficulties. Since ion implantation is a non-equilibrium process, it is not limited by solubility constraints or by surface chemistry. However, Er implantation does introduce considerable damage into the crystal lattice and post-implantation annealing is required. Wilson et al. [8] were the first to observe strong infrared luminescence, centered at 1.54  $\mu\text{m}$ , from Er-implanted GaN thin films. Co-implantation with O and furnace annealing were needed to achieve the strong luminescence. Several other research groups have also used ion implantation to dope GaN films with Er [9–11].

Three different methods of epitaxial growth have been successfully used for in situ doping of III–V nitride semiconductors with Er atoms: gas source Gen II metal-organic molecular beam epitaxy (MOMBE) [12], hydride vapor phase epitaxy (HVPE) [11], and solid source molecular beam epitaxy (MBE) [13]. However, with each of these techniques, there have been difficulties incorporating Er atoms into the epilayers and obtaining optically active centers. The maximum concentration of Er in these epilayers has been on the order of  $10^{20} \text{ cm}^{-3}$ . Nevertheless, high-quality epilayers, doped with Er ions, have been

achieved and good luminescence characteristics have been observed.

## 2. Optical excitation spectroscopy

Photoluminescence spectroscopy of the emission of Er-doped semiconductors involves optical excitation of the  $\text{Er}^{3+}$  ions and measurement of the light emission as a function of intensity and energy. It appears that three types of optical excitation are possible in the wide gap III–V nitride semiconductors. Using a laser source with above-bandgap photon energy, electron–hole pairs can be created in the semiconductor host. Some of the electron–hole pairs can transfer energy to the  $\text{Er}^{3+}$  ions, exciting the 4f-electrons to higher energy states, resulting in optical emission. Most of the PL measurements of Er-doped semiconductors have involved the use of a laser operating at an energy above that of the bandgap of the host semiconductor. This represents an indirect excitation of the  $\text{Er}^{3+}$  ions by electron–hole pairs. Recent studies have shown that defects in the semiconductor host can also serve as absorption centers transferring below-bandgap optical energy to the  $\text{Er}^{3+}$  ions [14,15]. This too corresponds to an indirect excitation of the  $\text{Er}^{3+}$  ions. A third method of optical excitation consists of resonant excitation of the  $\text{Er}^{3+}$  ions by the laser. In this case, the energy of the laser radiation is equal to that of one of the higher energy states of the  $\text{Er}^{3+}$  ion [16].

In Fig. 1 are the normalized room-temperature infrared PL spectra of different Er-doped III–V nitride films. The top spectrum is that for Er-implanted GaN; the middle one is that for Er-doped GaN grown on  $\text{Al}_2\text{O}_3$  substrate by MOMBE; and, the lower one is that for Er-doped AlN grown on  $\text{Al}_2\text{O}_3$  by MOMBE. All samples were excited with the 333.6–363.8 nm UV output of an Ar ion laser which corresponds to above-bandgap excitation. Each of the samples showed characteristic  $\text{Er}^{3+}$  emission centered at 1.54  $\mu\text{m}$ , which can be assigned to the intra-4f  $\text{Er}^{3+}$  transition  ${}^4I_{13/2} \rightarrow {}^4I_{15/2}$ . The PL spectra from in situ Er-doped GaN and AlN are very similar. They exhibit nearly featureless spectra with a full width half maximum (FWHM) of 25–35 nm suggesting a homogenous distribution of Er sites as typically observed from Er-doped glasses. The overall spectral width of the  $\text{Er}^{3+}$  emission from the Er-implanted GaN sample was significantly larger (100 nm at FWHM). Moreover, the Er-implanted GaN sample exhibited a more sharply structured  $\text{Er}^{3+}$  PL spectrum than the in situ Er-doped samples. Based on previous data, the more complex and broader  $\text{Er}^{3+}$  PL spectrum seems to be characteristic for Er-implanted GaN samples and is due to a combination of different Er sites and Stark splitting of energy levels in low-symmetry sites. For example, Kim et al. identified up to four different Er sites in Er-implanted GaN grown by MOCVD [10]. Time-resolved PL studies of in situ Er-doped AlN (MOMBE)

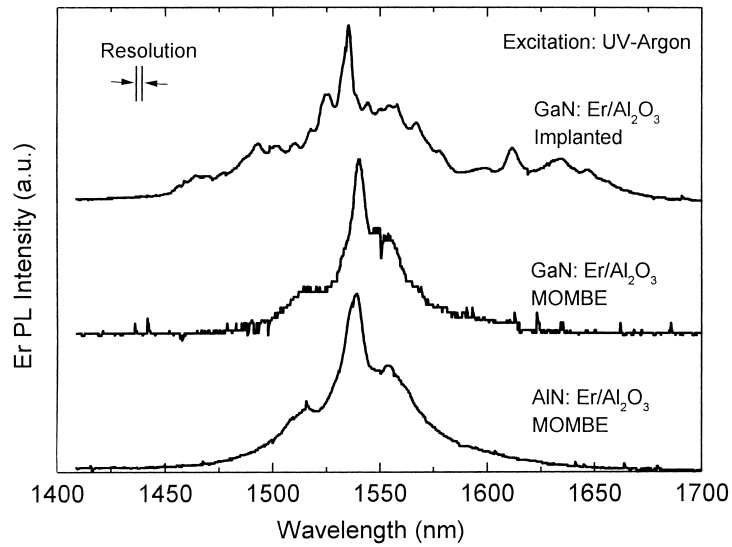


Fig. 1. Room-temperature  $\text{Er}^{3+}$  PL spectra of Er-doped III-V nitride films: Top, Er-implanted GaN; Middle, in situ Er-doped GaN grown by MOMBE; and Lower, Er-doped AlN grown by MOMBE.

have indicated the existence of at least two different classes of  $\text{Er}^{3+}$  sites with distinct lifetime and excitation schemes [17].

We performed a series of experiments to determine the thermal quenching of luminescence in the Er-implanted GaN films [14]. The GaN films, which were grown on sapphire substrates, were co-implanted at room temperature with Er and O ions. The  $\text{Er}^{3+}$  emission in the region of  $1.54 \mu\text{m}$  was measured over the temperature range 13–550 K. For temperature-dependent measurements between 15 and 300 K, the Er-implanted GaN sample was placed onto a cold finger of a closed-cycle helium refrigerator. For measurements above 300 K, a specially

made heating element was used. The sample was excited with above-bandgap radiation, using a HeCd laser operating at 325 nm, and with below-bandgap radiation, using an Ar ion laser operating at 488 nm. In Fig. 2(a) are shown the high-resolution PL spectra at 300 and 550 K of the sample pumped with above-bandgap excitation. There were only minor changes in the PL spectra between 300 and 550 K. The FWHM of the PL spectrum at 300 K was  $\sim 80 \text{ nm}$ , suggesting inhomogeneous broadening of the emission. This broadening indicated that the  $\text{Er}^{3+}$  ions occupy a range of sites, with slightly different atomic configurations, in the GaN host. The integrated PL intensity of the luminescence was found to be nearly

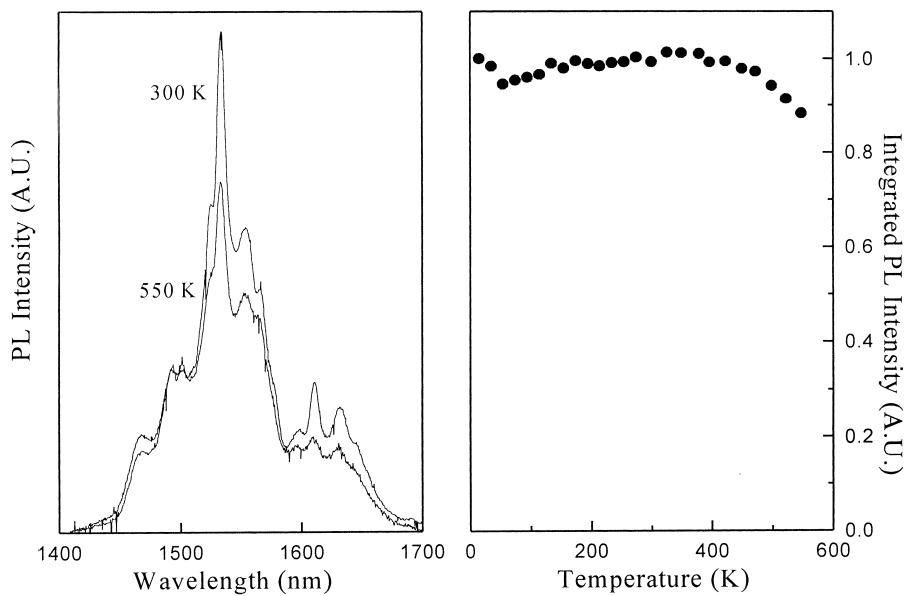


Fig. 2. Above-bandgap photoluminescence spectrum of Er-implanted GaN at 300 K and 550 K. The integrated PL intensity was found to be nearly temperature independent up to 550 K.

over the entire range of measurement temperatures, see Fig. 2(b). Relative to its value at 15 K, the integrated PL intensity at 550 K decreased by only about 10%. This remarkable temperature stability of the  $\text{Er}^{3+}$  luminescence is the best reported data from any Er-doped semiconductor, including Er-doped SiC [18].

In Fig. 3(a) are shown the high-resolution PL spectra at 300 and 550 K of the sample excited by below-bandgap radiation. This excitation method corresponds to indirect excitation of the  $\text{Er}^{3+}$  ions through the broad, defect-related, absorption band. There were significant changes in the PL spectrum between 300 and 550 K. In addition, depending upon the excitation method, different subsets of  $\text{Er}^{3+}$  ions are excited leading to distinct PL spectra, as shown in Figs. 2(a) and 3(a). The FWHM of the PL spectrum in Fig. 3(a) at 300 K was  $\sim 50$  nm, which was narrower than that in Fig. 2(a). There was also a large change in the integrated PL intensity over the range of measurement temperatures, as indicated in Fig. 3(b). Relative to its value at 15 K, the integrated PL intensity at 550 K decreased by about 50%. While this behavior is not as good as the data shown in Fig. 2(b), this reduced thermal quenching is still less than that reported from any other Er-doped III–V semiconductor.

Large improvements of the absolute  $\text{Er}^{3+}$  PL intensity have been observed for Er-doped Si and GaAs samples that were co-doped with oxygen. The enhanced  $1.54 \mu\text{m}$  PL was attributed to an increased concentration of optically active  $\text{Er}^{3+}$  ions and a more efficient  $\text{Er}^{3+}$  PL excitation process. A similar improvement in the  $\text{Er}^{3+}$  PL intensity was observed in the Er-implanted GaN sample

under below-gap excitation [8]. We performed a study of the effect of O and C impurities on the PL intensity of Er-doped GaN films grown by MOMBE on (111) Si or (0001) sapphire substrates. The GaN films were preceded by a low-temperature AlN buffer growth ( $T_g = 425^\circ\text{C}$ ) and a  $0.2 \mu\text{m}$  undoped GaN spacer layer prior to the deposition of the GaN:Er film. Triethylgallium (TEGa), dimethylethylamine alane (DMEAA), and thermally evaporated 8 N Ga metal were used to provide the group III fluxes. A shuttered effusion oven with 4 N Er was used for solid source doping. Due to the residual ether in TEGa, O and C background levels were very high in TEGa derived GaN films. Concentrations of  $[\text{O}] \sim 10^{20} \text{ cm}^{-3}$  and  $[\text{C}] \sim 10^{21} \text{ cm}^{-3}$  were determined through SIMS analysis. GaN films grown using thermally evaporated 8 N pure Ga as the group III source had O and C backgrounds of less than  $10^{19} \text{ cm}^{-3}$ . The absolute  $\text{Er}^{3+}$  PL intensities of the different GaN:Er films were measured under below-gap and above-gap excitation. A comparison of the PL spectra is depicted in Fig. 4. With below-gap excitation, the GaN:Er (TEGa) sample, having a high O and C background, showed a peak PL intensity nearly two orders of magnitude larger than the GaN:Er (Ga) sample, with low O and C backgrounds. It is interesting to note that the GaN:Er (TEGa) sample grown on a Si substrate showed a strong  $1.54 \mu\text{m}$  PL at room temperature, which makes this material combination attractive for integration with Si-based optoelectronics. The results for below-gap excitation [Fig. 4(a)] indicate that the incorporation of O and C introduces beneficial mid-gap states which provide efficient excitation pathways to the  $\text{Er}^{3+}$  ions. The visible

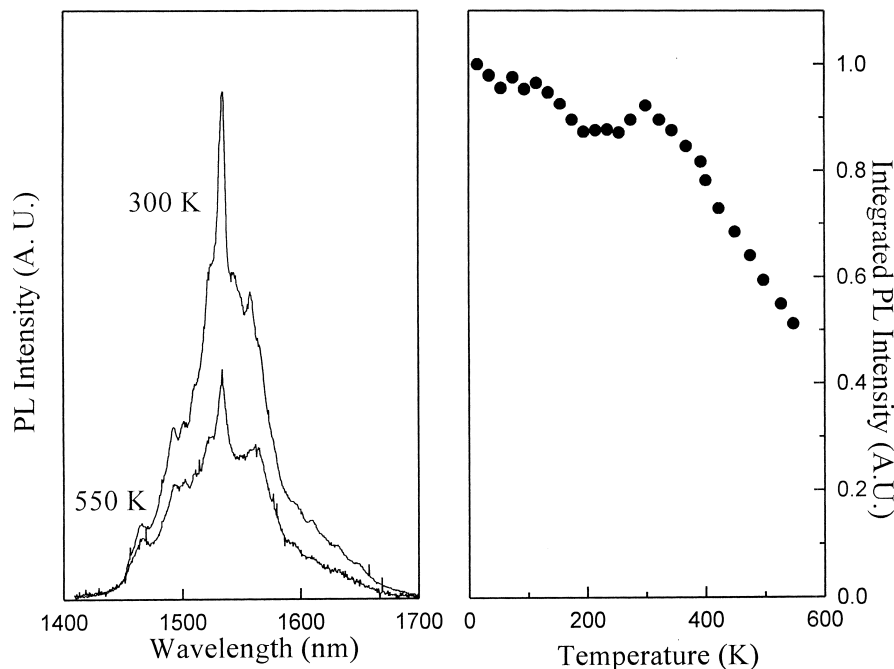


Fig. 3. Below-bandgap photoluminescence spectrum of Er-implanted GaN at 300 K and 550 K. The integrated PL intensity was found to be nearly temperature independent up to 300 K.

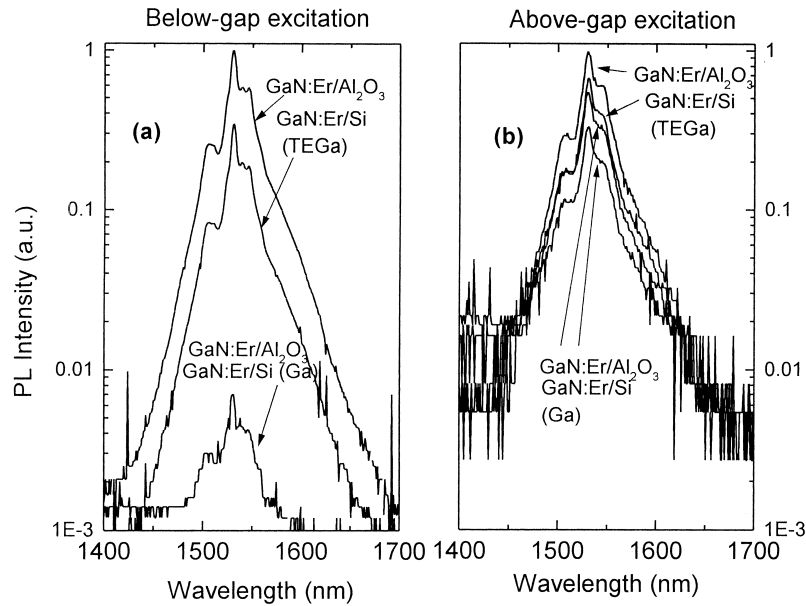


Fig. 4. Comparison of the absolute  $\text{Er}^{3+}$  PL intensity from different Er-doped GaN (MOMBE) samples for: (a) below-bandgap excitation; and (b) above-bandgap excitation. Only the PL spectra taken with below-bandgap excitation show a significant dependence on high concentrations of O and C impurities.

output from the Ar ion laser leads to a significantly more efficient excitation of  $\text{Er}^{3+}$  in the GaN:Er/Si (TEGa) samples than in the GaN: Er/Si (Ga) samples.

With above-gap excitation [Fig. 4(b)] all of the GaN:Er (MOMBE) samples showed a greatly reduced  $\text{Er}^{3+}$  PL intensity relative to below-gap excitation, independent of O and C concentration. A similar PL reduction was reported for Er-implanted GaN [10]. It is somewhat surprising that under above-gap excitation the  $\text{Er}^{3+}$  PL intensity of samples with high O and C background levels

was only roughly twice as strong as the  $\text{Er}^{3+}$  PL observed from samples with low O and C contents. The data indicate that high O and C concentrations do not necessary lead to an enhanced luminescence for carrier-mediated  $\text{Er}^{3+}$  excitation.

However, high O and C concentrations do affect the thermal quenching characteristics of the Er-doped GaN films. In Fig. 5 the behavior of the integrated  $\text{Er}^{3+}$  PL intensity is shown for the temperature range from 15 to 500 K. With below-gap excitation significantly different

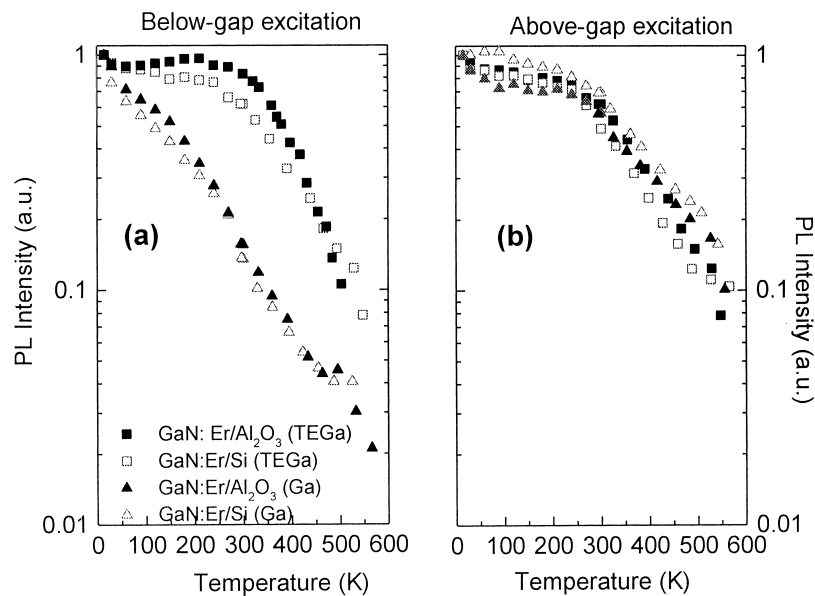


Fig. 5. Temperature dependence of the integrated PL intensity from in situ Er-doped GaN grown by MOMBE for: (a) below-bandgap excitation; and (b) above-bandgap excitation.

$\text{Er}^{3+}$  PL quenching characteristics were observed for samples with varying O and C contents [Fig. 5(a)]. As previously observed for Si:Er and GaAs:Er samples codoped with O, the GaN:Er samples with high O and C concentrations showed a significantly reduced  $\text{Er}^{3+}$  PL quenching compared to samples with low O and C backgrounds. Between 15 K and room-temperature, GaN:Er samples with high O and C backgrounds showed  $\text{Er}^{3+}$  PL quenching of only  $\sim 20\%$ , whereas the  $1.54 \mu\text{m}$  luminescence from low O and C concentration samples decreased by  $\sim 90\%$  over the same temperature range. With above-gap excitation the situation was different. As shown in Fig. 5(b), hardly any difference was observed in the  $\text{Er}^{3+}$  PL quenching behavior for samples with varying O and C levels. The O and C concentration does not appear to greatly effect the carrier-mediated  $\text{Er}^{3+}$  excitation. Up to room temperature, the  $\text{Er}^{3+}$  PL decreased for all four samples by less than 50% relative to its low-temperature value. At 550 K, the  $\text{Er}^{3+}$  PL from all samples had decreased by nearly 90% of its low-temperature value.

Recently, Steckl et al. reported strong visible (green) PL from in situ Er-doped GaN grown by MBE on sapphire and Si substrates [19]. Solid sources were used to supply the Ga and Er fluxes, while a STVA radio-frequency (RF) plasma source supplied atomic nitrogen. With above-bandgap excitation, the PL spectrum consisted of peaks in the visible region at 537 and 558 nm corresponding to Er-related transitions from the  $^2H_{11/2}$  and the  $^4S_{3/2}$  levels to the  $^4I_{15/2}$  ground state. The FWHM of the  $^2H_{11/2} \rightarrow ^4I_{15/2}$  and  $^4S_{3/2} \rightarrow ^4I_{15/2}$  lines were 2.56 and 3.0 nm, respectively. The data represented the first visible emissions from any Er-doped GaN film under optical excitation. Based on these results, Er-doped GaN LEDs emitting in both the visible and IR regions were fabricated [20]. The GaN:Er LEDs consisted of Schottky diodes which used a transparent indium tin oxide (ITO) layer for both positive and negative electrodes. Strong Er-activated, green emission was observed under reverse bias conditions. The overall efficiency of the green emission was estimated at  $2 \times 10^{-5}$  which is comparable to that from Er-doped Si emission at  $1.54 \mu\text{m}$  [21].

Further evidence of the influence of the Er-doping method on the resulting  $\text{Er}^{3+}$  emission is presented in Fig. 6. An absolute intensity comparison of the emission at  $1.54 \mu\text{m}$  was made between one of the GaN:Er samples (71005-1) prepared by MOMBE and one of the GaN:Er samples (102R) prepared by MBE. Both samples were grown on Si substrates and excited both by below-bandgap and by above-bandgap radiation. In Fig. 6(a) are shown the PL spectra at 300 K of the samples excited by below-bandgap radiation at 442 nm from a HeCd laser. While the emission from the MOMBE sample is nearly twice as intense as that from the MBE sample, the general features of the two spectra are very similar. However, when the samples were excited by above-bandgap radiation at 325 nm from the HeCd laser, significant changes in the PL

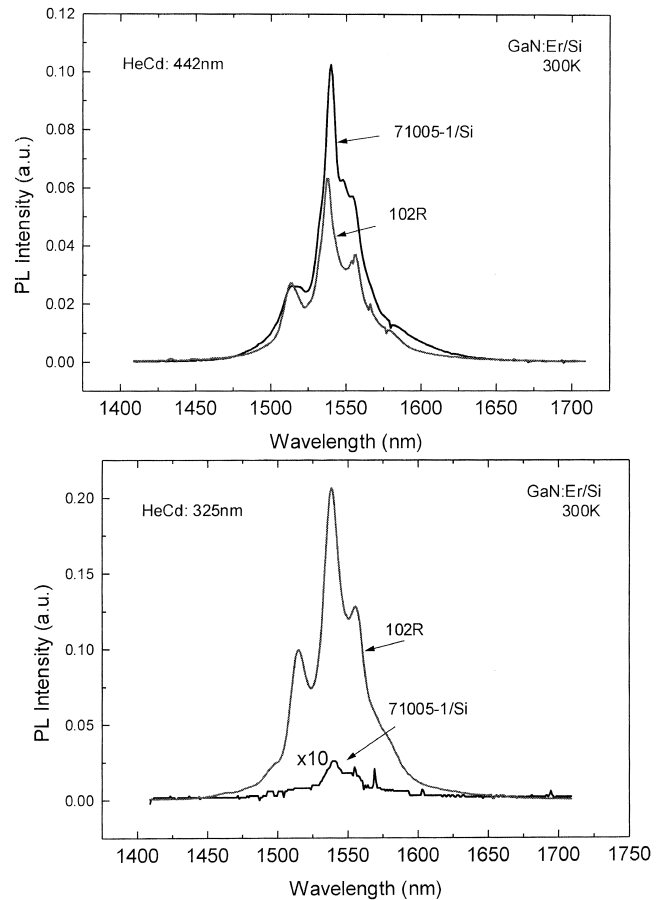


Fig. 6. Comparison of the absolute  $\text{Er}^{3+}$  PL intensity at 300 K from Er-doped GaN films grown by MOMBE (71015-1) and by MBE (102R). The PL spectra are for: (a) below-bandgap excitation; and (b) above-bandgap excitation.

spectra were observed, see Fig. 6(b). The emission from the MBE sample is about two orders more intense than that from the MOMBE sample. In addition, the general features of the two spectra are very different. Furthermore, with above-bandgap excitation, the GaN:Er sample (102R), prepared by MBE, showed bright green emission whereas the GaN:Er sample prepared by MOMBE did not. It seems safe to conclude that different  $\text{Er}^{3+}$  complexes are produced during the two different growth techniques resulting in very different absorption and emission properties.

### 3. Summary

Considerable progress has been made in the past 10 years in understanding the optical properties of Er-doped III–V semiconductors. Luminescence of  $\text{Er}^{3+}$  ions in many III–V semiconductors has been observed. A number of experiments have shown that the use of wide gap semiconductors, such as the III–V nitrides, significantly reduces the thermal quenching of the  $\text{Er}^{3+}$  luminescence. However, difficulties remain concerning the incorporation of Er

atoms in the III–V nitride materials and the proper processing conditions necessary for optical activation. Furthermore, different Er-doping techniques lead to different emission spectra with different thermal quenching characteristics. Due to the intense current research in III–V nitride semiconductors for blue light emission, major improvements in the crystal quality and in the processing technology of these materials are very likely to occur. Such advances will assist efforts to develop devices based on III–V nitride semiconductors doped with Er ions, making possible a new class of optoelectronic components for optical communication and display systems.

### Acknowledgements

The authors would like to thank A. J. Steckl for the loan of the GaN:Er sample grown by MBE which permitted the PL experiments described in Fig. 6.

### References

- [1] W. Koechner, Solid State Laser Engineering, 3rd Edition, Springer Verlag, 1992.
- [2] E. Desurvire, J.R. Simpson, P.C. Becker, Opt. Lett. 12 (1987) 888.
- [3] H. Ennen, J. Schneider, G. Pomrenke, A. Axmann, Appl. Phys. Lett. 43 (1983) 943.
- [4] G.S. Pomeroy, P.B. Klein, D.W. Langer (Eds.), Rare Earth Doped Semiconductors I, Materials Research Society Proc., Vol. 301, 1993.
- [5] J.M. Zavada, D. Zhang, Solid-State Electron. 38 (1995) 1285.
- [6] S. Coffa, A. Polman, R.N. Schwartz (Eds.), Rare Earth Doped Semiconductors II, Materials Research Society Proc., Vol. 422, 1996.
- [7] P.N. Favenec, H. L'Haridon, M. Salvi, D. Moutonnet, Y.L. Guillou, Electron. Lett. 25 (1989) 718.
- [8] R.G. Wilson, R.N. Schwartz, C.R. Abernathy, S.J. Pearton, N. Newman, M. Rubin, T. Fu, J.M. Zavada, Appl. Phys. Lett. 65 (1994) 992.
- [9] J.T. Torvik, R.J. Feuerstein, J.I. Pankove, C.H. Qiu, F. Namavar, Appl. Phys. 69 (1996) 2098.
- [10] S. Kim, S.J. Rhee, D.A. Turnbull, E.E. Reuter, X. Li, J.J. Coleman, S.G. Bishop, Appl. Phys. Lett. 71 (1997) 231.
- [11] D.M. Hansen, R. Zhang, N.R. Perkins, S. Safvi, L. Zhang, K.L. Bray, T.F. Keuch, Appl. Phys. Lett. 72 (1997) 1244.
- [12] J.D. MacKenzie, C.R. Abernathy, S.J. Pearton, U. Hömmerich, X. Wu, R.N. Schwartz, R.G. Wilson, J.M. Zavada, Appl. Phys. Lett. 69 (1996) 2083.
- [13] A.J. Steckl, R. Birkhahn, Appl. Phys. Lett. 73 (1998) 1701.
- [14] Myo Thaik, U. Hömmerich, R.N. Schwartz, R.G. Wilson, J.M. Zavada, Appl. Phys. Lett. 71 (1997) 2641.
- [15] S. Kim, S.J. Rhee, D.A. Turnbull, E.E. Reuter, X. Li, J.J. Coleman, S.G. Bishop, P.B. Klein, Appl. Phys. Lett. 71 (1997) 2662.
- [16] J.T. Torvik, R.J. Feuerstein, C.H. Qiu, M.W. Leksano, F. Namavar, J.I. Pankove, Mat. Res. Soc. Symp. Proc. 422 (1996) 199.
- [17] X. Wu, U. Hömmerich, J.D. MacKenzie, C.R. Abernathy, S.J. Pearton, R.N. Schwartz, R.G. Wilson, J.M. Zavada, Appl. Phys. Lett. 70 (1997) 2126.
- [18] W.J. Choyke, R.P. Devaty, L.I. Clemen, M. Yoganathan, G. Pensl, Ch. Hassler, Appl. Phys. 65 (1994) 1668.
- [19] A.J. Steckl, R. Birkhahn, Appl. Phys. Lett. 73 (1998) 1700.
- [20] A.J. Steckl, M. Garter, R. Birkhahn, J. Scofield, Appl. Phys. Lett. 73 (1998) 2450.
- [21] F. Priolo, S. Coffa, G. Franzo, A. Polman, Mat. Res. Soc. Symp. Proc. 422 (1996) 305.